Geosci. Model Dev. Discuss., 7, 7317–7349, 2014
www.geosci-model-dev-discuss.net/7/7317/2014/
doi:10.5194/gmdd-7-7317-2014
© Author(s) 2014. CC Attribution 3.0 License.

Geoscientific Model Development Discussions
Open Access

This discussion paper is/has been under review for the journal Geoscientific Model Development (GMD). Please refer to the corresponding final paper in GMD if available.

Simulation of groundwater and surface water over the continental US using a hyperresolution, integrated hydrologic model

R. M. Maxwell[1], L. E. Condon[1], and S. J. Kollet[2]

[1]Hydrologic Science and Engineering Program, Integrated GroundWater Modeling Center, Department of Geology and Geological Engineering, Colorado School of Mines, Golden, Colorado, USA
[2]Centre for High-Performance Scientific Computing in Terrestrial Systems, Institute for Bio- and Geosciences, Agrosphere (IBG-3), Research Centre Jülich, Jülich, Germany

Received: 11 October 2014 – Accepted: 16 October 2014 – Published: 4 November 2014

Correspondence to: R. M. Maxwell (rmaxwell@mines.edu)

Published by Copernicus Publications on behalf of the European Geosciences Union.

Abstract

Interactions between surface and groundwater systems are well-established theoretically and observationally. While numerical models that solve both surface and subsurface flow equations in a single framework (matrix) are increasingly being applied, computational limitations have restricted their use to local and regional studies. Regional or watershed, scale simulations have been effective tools in understanding hydrologic processes, however there are still many questions, such as the adaptation of water resources to anthropogenic stressors and climate variability, that need to be answered across large spatial extents at high resolution. In response to this "grand challenge" in hydrology, we present the results of a parallel, integrated hydrologic model simulating surface and subsurface flow at high spatial resolution (1 km) over much of continental North America ($\sim$ 6 300 000 or 6.3 million km^2). These simulations provide predictions of hydrologic states and fluxes, namely water table depth and streamflow, at unprecedented scale and resolution. The physically-based modeling approach used here requires limited parameterizations and relies only on more fundamental inputs, such as topography, hydrogeologic properties and climate forcing. Results are compared to observations and provide mechanistic insight into hydrologic process interaction. This study demonstrates both the feasibility of continental scale integrated models and their utility for improving our understanding of large-scale hydrologic systems; the combination of high resolution and large spatial extent facilitates novel analysis of scaling relationships using model outputs.

1 Introduction

There is growing evidence of feedbacks between groundwater, surface water and soil moisture that moderate land-atmospheric energy exchanges, and impact weather and climate (Maxwell et al., 2007, 2011; Anyah et al., 2008; Kollet and Maxwell, 2008; Maxwell and Kollet, 2008; Jiang et al., 2009; Rihani et al., 2010; Williams and Maxwell,

GMDD
7, 7317–7349, 2014

CC BY

2011; Condon et al., 2013; Taylor et al., 2013). While local observations and remote sensing can now detect changes in the hydrologic cycle from small to very large spatial scales (e.g. Rodell et al., 2009), theoretical approaches to connect and scale hydrologic states and fluxes from point measurements to the continental scales are incomplete. In this work we present integrated modeling as one means to bridge this gap.

Though introduced as a concept in the literature almost half a century ago (Freeze and Harlan, 1969), integrated hydrologic models that solve the surface and subsurface systems simultaneously have only been a reality for about a decade (VanderKwaak and Loague, 2001; Jones et al., 2006; Kollet and Maxwell, 2006). Since their implementation, integrated hydrologic models have been successfully applied to a wide range of watershed-scale studies (see Table 1 in Maxwell et al., 2014) successfully capturing observed surface and subsurface behavior (Qu and Duffy, 2007; Jones et al., 2008; Sudicky et al., 2008; Camporese et al., 2010; Shi et al., 2013), diagnosing stream-aquifer and land-energy interactions (Maxwell et al., 2007; Kollet and Maxwell, 2008; Rihani et al., 2010; Condon et al., 2013; Camporese et al., 2014), and building our understanding of the propagation of perturbations such as land-cover and anthropogenic climate change throughout the hydrologic system (Maxwell and Kollet, 2008; Goderniaux et al., 2009; Sulis et al., 2012; Mikkelson et al., 2013).

Prior to this work, computational demands and data constraints have limited the application of integrated models to regional domains. Advances in parallel solution techniques, numerical solvers, supercomputer hardware and additional data sources have only recently made large-scale, high-resolution simulation of the terrestrial hydrologic cycle technically feasible (Kollet et al., 2010; Maxwell, 2013). As such, existing large scale studies of the subsurface have focused on modeling groundwater independently (Fan et al., 2007, 2013; Miguez-Macho et al., 2007;) and classifying behavior with analytical functions (Gleeson et al., 2011a). Similarly, continental scale modeling of the surface water has utilized tools with simplified groundwater systems that do not capture lateral groundwater flow and model catchments as isolated systems (Maurer et al., 2002; Döll et al., 2012; Xia et al., 2012). Despite the fact that lateral flow of

GMDD
7, 7317–7349, 2014

CC BY

groundwater has been shown to be important across scales (Nir et al., 2014). While much has been learned from previous studies, the focus on isolated components within what we know to be an interconnected hydrologic system is a limitation than can only be addressed with an integrated approach.

The importance of groundwater surface water interactions in governing scaling behavior of surface and subsurface flow from headwaters to the continent has yet to be fully characterized. Indeed, one of the purposes for building an integrated model is to better understand and predict the nature of hydrologic connections across scales and throughout a wide array of physical and climate settings. Arguably, this is not possible utilizing observations, because of data scarcity and challenges observing 3-D groundwater flow across a wide range of scale. For example, the scaling behavior of river networks is well known (Rodriguez-Iturbe and Rinaldo, 2001), yet open questions remain about the quantity, movement, travel time, and spatial and temporal scaling of groundwater and surface water at the continental scale. Exchange processes and flow near the land surface are strongly non-linear, and heterogeneity in hydraulic properties exist at all spatial scales. As such, a formal framework for connecting scales in hydrology (Wood, 2009) needs to account for changes in surface water and groundwater flow from the headwaters to the mouth of continental river basins. We propose that integrated, physics-based hydrologic models are a tool for providing this understanding, solving fundamental non-linear flow equations at high spatial resolution while numerically scaling these physical processes up to a large spatial extent, i.e. the continent.

In this study, we simulate surface and subsurface flow at high spatial resolution (1 km) over much of continental North America ($\sim$ 6 300 000 or 6.3 million km^2), which is itself considered a grand challenge in hydrology (e.g. Wood et al., 2011; Gleeson and Cardiff, 2014). This simulation solves surface and subsurface flow simultaneously and takes full advantage of massively parallel, high-performance computing. The domain is constructed entirely of available datasets including topography, soil texture and hydrogeology. Results are compared to observations, and used to diagnose physical behavior and evaluate scaling relationships. The paper is organized as follows: first a brief

GMDD
7, 7317–7349, 2014

CC BY

description of the model equations are provided including a description of the input variables and observational datasets used for model comparison; next model simulations are compared to observations in a number of ways, and then used to understand hydrodynamic characteristics and to describe scaling.

2 Methods

The model was constructed using the integrated simulation platform ParFlow (Ashby and Falgout, 1996; Jones and Woodward, 2001; Kollet and Maxwell, 2006) utilizing the terrain following grid capability (Maxwell, 2013). ParFlow is a physically based model that solves both the surface and subsurface systems simultaneously. In the subsurface ParFlow solves the mixed form of Richards' equation for variably saturated flow (Richards, 1931) in three spatial dimensions given as:

$$S_s S_w(h)\frac{\partial h}{\partial t} + \phi S_w(h)\frac{\partial S_w(h)}{\partial t} = \nabla \cdot \boldsymbol{q} + q_r(x,z) \quad (1)$$

where the flux term $\boldsymbol{q}$ [L T^{-1}] is based on Darcy's law:

$$\boldsymbol{q} = -\mathbf{K}_s(\boldsymbol{x})k_r(h)[\nabla(h+z)\cos\theta_x + \sin\theta_x] \quad (2)$$

In these expressions, h is the pressure head [L]; z is the elevation with the z axis specified as upward [L]; $\mathbf{K}_s(\boldsymbol{x})$ is the saturated hydraulic conductivity tensor [L T^{-1}]; k_r is the relative permeability [–]; S_s is the specific storage [L^{-1}]; φ is the porosity [–]; S_w is the relative saturation [–]; q_r is a general source/sink term that represents transpiration, wells, and other fluxes [T^{-1}]; and θ [–] is the local angle of slope, in the x and y directions and may be written as $\theta_x = \tan^{-1} S_x$ and $\theta_y = \tan^{-1} S_y$. Note that we assume that density and viscosity are both constant, though this assumption is not necessarily needed in ParFlow (Kollet et al., 2009). The van Genuchten (1980) relationships are used to describe the relative saturation and permeability functions

GMDD
7, 7317–7349, 2014

($S_w(h)$ and $k_r(h)$ respectively). These functions are highly nonlinear and characterize changes in saturation and permeability with pressure.

Overland flow is represented in ParFlow by the two-dimensional kinematic wave equation resulting from application of continuity conditions for pressure and flux (Kollet and Maxwell, 2006):

$$\boldsymbol{k} \cdot (-\mathbf{K}_s(\boldsymbol{x}) k_r(h) \cdot \nabla(h+z)) = \frac{\partial \|h,0\|}{\partial t} - \nabla \cdot \|h,0\| \boldsymbol{v}_{sw} + \lambda q_r(\boldsymbol{x}) \quad (3)$$

In this equation $\boldsymbol{v}_{sw}$ is the two-dimensional, depth-averaged surface water velocity [LT^{-1}] given by manning's equation; h is the surface ponding depth [L] the same h as is shown in Eq. (1). Note that $\|h,0\|$ indicates the greater value of the two quantities in Eq. (3). This means that if $h<0$ the left hand side of this equation represents vertical fluxes (e.g. in/exfiltration) across the land surface boundary and is equal to $q_r(\boldsymbol{x})$ and a general source/sink (e.g. rainfall, ET) rate [LT^{-1}] with λ being a constant equal to the vertical grid spacing [L^{-1}]. This term is then entirely equivalent to the source/sink term shown in Eq. (1) at the ground surface where $\boldsymbol{k}$ is the unit vector in the vertical, again defining positive upward coordinates. If $h>0$ then the terms on the right hand side of Eq. (3) are active water that is routed according to surface topography (Kollet and Maxwell, 2006).

The nonlinear, coupled equations of surface and subsurface flow presented above are solved in a fully-implicit manner using a parallel Newton–Krylov approach (Jones and Woodward, 2001; Kollet and Maxwell, 2006; Maxwell, 2013). Utilizing a globally-implicit solution allows interactions between the surface and subsurface flow system to be explicitly resolved. While this yields a very challenging computational problem, ParFlow is able to solve large complex systems by utilizing a multigrid preconditioner (Osei-Kuffuor et al., 2014; Ashby and Falgout, 1996) and taking advantage of highly scaled parallel efficiency out to more than 1.6×10^4 processors (Kollet et al., 2010; Maxwell, 2013).

Physically this means that ParFlow solves saturated subsurface flow (i.e. groundwater), unsaturated subsurface flow (i.e. the vadose zone) and surface flow (i.e.

GMDD
7, 7317–7349, 2014

streamflow) in a continuum approach within a single matrix. Thus, complete non-linear interactions between all system components are simulated without a priori specification of what types of flow occur in any given portion of the grid. Streams form purely based on hydrodynamic principles governed by recharge, topography, hydraulic conductivity and flow parameters, when water is ponded due to either excess infiltration (surface fluxes exceed the infiltration capacity) or excess saturation (subsurface exfiltration to the surface system). Groundwater converges in topographic depressions and unsaturated zones may be shallow or deep depending upon recharge and lateral flows.

The physically based approach used by ParFlow is similar to other integrated hydrologic models such as Hydrogeosphere (Therrien et al., 2012), PIHM (Kumar et al., 2009) and CATHY (Camporese et al., 2010). This is a distinct contrast with more conceptually-based models that may not simulate lateral groundwater flow or may simplify the solution of surface and subsurface flow by defining regions of groundwater or the stream-network, prior to the simulation. In such models, groundwater surface water interactions are often captured as one-way exchanges (i.e. surface water loss to groundwater) or parameterized with simple relationships (i.e. curves to impose the relationship between stream head and baseflow). The integrated approach used by ParFlow eliminates the need for such assumptions and allows the interconnected groundwater surface water systems to evolve dynamically based only on the governing equations and the properties of the physical system. The approach used here requires robust numerical solvers and exploits high-performance computing to achieve high resolution, large extent simulations.

3 Domain setup

In this study, the model for the Continental US (CONUS) was constructed using the terrain following grid framework (Maxwell, 2013) for a total thickness of 102 m over 5 model layers. The model was implemented with a lateral resolution of 1 km with nx = 3342, ny = 1888 and five vertical layers with 0.1, 0.3, 0.6, 1.0 and 100 m discretization for a total model dimensions of 3342 by 1888 by 0.102 km and 31 548 480 total compute cells. The model domain and input data sets are shown in Fig. 1. All model inputs were re-projected to have an equal cell-size of 1 km as shown in Fig. 1. Topographic slopes (S_x and S_y) were calculated from the Hydrosheds digital elevation model (Fig. 1b) and were processed using the r.watershed package in the GRASS GIS platform. Over the top 2 m of the domain, hydraulic properties from soil texture information of SSURGO were applied and soil properties were obtained from Schaap and Leij (1998). Note that two sets of soil categories were available. The upper horizon was applied over the top 1 m (the top three model layers) and the bottom one over the next 1 m (the fourth model layer). Figure 1a and c show the top and bottom soil layers of the model. The deeper subsurface (i.e. below 2 m) was constructed from a global permeability map developed by Gleeson et al. (2011b). These values (Gleeson et al., 2011b) were adjusted to reduce variance (Condon and Maxwell, 2013, 2014) and to reflect changes in topography using the e-folding relationship empirically-derived in Fan et al. (2007): $\alpha = e^{-\frac{50}{f}}$ where $f = \frac{a}{\left(1+b\cdot\sqrt{S_x^2+S_y^2}\right)}$. For this analysis $a = 20$, $b = 125$ and the value of 50 [m] was chosen to reflect the midpoint of the deeper geologic layer in the model. Larger values of α reduced the hydraulic conductivity categorically, that is by decreasing the hydraulic conductivity indicator values in regions of steeper slope. Figure 1e maps the final conductivity values used for simulation. Note that this complex subsurface dataset is assembled from many sources. As such, there are breaks across dataset boundaries, commonly at State or Province and International political delineations. The fidelity and resolution of the source information used to formulate this dataset also changes across these boundaries yielding some interfaces in property values. All input datasets are a work in progress and should be continually improved. Still, we feel it is important to continue modeling with the data that is currently available to understand limitations and assess their impact on model predictions. Shortcomings in hydrogeological data sets reflect the lack of detailed and unified hydrogeological information that can be applied in high resolution continental models.

GMDD
7, 7317–7349, 2014

CC BY

No-flow boundary conditions were imposed on all sides of the model except the land surface, where the free-surface overland flow boundary condition was applied. For the surface flux, a Precipitation-Evapotranspiration (P-E, or potential recharge) product was derived from a combination of precipitation and model-simulated evaporation and transpiration fluxes for a product very similar to Maurer et al. (2002), shown in Fig. 1d. The model was initialized dry and the P-E forcing was applied continuously at the land surface until the balance of water (difference between total outflow and P-E) was less than 3 % of storage.

While this study employs state of the art modeling techniques, it is important to note that the numerical simulation of this problem is still non-trivial. Simulations were split over 128 divisions in the x direction and 128 in the y direction and run on 16 384 compute-cores of an IBM BG/Q supercomputer (JUQUEEN) located at the Jülich Supercomputing Centre, Germany. These processor splits resulted in approximately 2000 unknowns per compute core; a relatively small number, yet ParFlow's scaling was still good due to the non-symmetric preconditioner used (Maxwell, 2013). Additionally, code performance was improved using efficient preconditioning of the linear system (Osei-Kuffuor et al., 2014). The steady-state flow field was accomplished over several steps. Artificial dampening was applied to the overland flow equations early in the simulation during water table equilibration. Dampening was subsequently decreased and removed entirely as simulation time progressed. Large time steps (10 000 h) were used initially and were decreased (to 1 h) as the stream network formed and overland flow became more pronounced with reduced dampening. The entire simulation utilized approximately 2.5 million core hours of compute time, which resulted in less than 1 week of wall-clock time (approximately 150 h) given the large core counts and batch submission process.

Model results were validated against available observations of streamflow and hydraulic head (the sum of pressure head and gravitational potential). Observed streamflow values were extracted from a spatial dataset of current and historical US Geological Survey (USGS) stream gages mapped to the National Hydrography Dataset (NHD)

CC BY

(Stewart et al., 2006). The entire dataset includes roughly 23 000 stations, of which just over half (13 567) fall within the CONUS domain. For each station, the dataset includes location, drainage area, sampling time period and flow characteristics including minimum, maximum, mean and a range of percentiles (1, 5, 10, 20, 25, 50, 75, 80, 90, 95, 99) compiled from the USGS gage records. For comparison, stations without a reported drainage area, stations not located on or adjacent to a river cell in ParFlow, and stations whose drainage area were not within twenty percent of the calculated ParFlow drainage area were filtered out. This resulted in 4736 stations for comparison. The 50th percentile values for these stations are shown in Fig. 2a. Note that these observations are not naturalized, i.e. no attempt is made to remove dams and diversions along these streams and rivers, however some of these effects will be minimized given the longer temporal averages. Hydraulic head observations of groundwater at more than 160 000 locations were assembled by Fan et al. (2007, 2013). Figure 2b plots the corresponding water table depth at each location calculated as the difference between elevation and hydraulic head. Note that these observations include groundwater pumping (most wells are drilled for extraction rather than purely observation).

4 Results and discussion

Figures 3 and 4 plot simulated streamflow and water table depth, respectively, over much of continental North America, both on a log scale for flow (Fig. 3) and water table depth (Fig. 4). Figure 3 shows a complex stream network with flow rates spanning many orders of magnitude. Surface flows originate in the headwaters (or recharge zones) creating tributaries that join to form the major river systems in North America. Note, as discussed previously, that the locations for flowing streams are not enforced in ParFlow but form due to ponded water at the surface (i.e. values of $h > 0$ in the top layer of the model in Eqs. 1–3). Overland flow is promoted both by topographic convergence, and surface and subsurface flux; however, with this formulation there is no requirement that all potential streams support flow. Thus, the model novelly captures the generation

GMDD
7, 7317–7349, 2014

of the complete stream network without specifying the presence and location of rivers in advance, but rather by allowing channelized flow to evolve as a result of explicitly simulated non-linear physical processes.

The insets in Fig. 3 demonstrate multiscale detail ranging from the continental river systems to the first-order headwaters. In Fig. 4, water table depth also varies over five orders of magnitude. Whereas aridity drives large-scale differences in water table depth (Fig. 1d), at smaller scales, lateral surface and subsurface flow processes clearly dominate recharge and subsurface heterogeneity (see insets to Fig. 4). Water tables are deeper in the more arid western regions, and shallower in the more humid eastern regions of the model. However, areas of shallow water table exist along arid river channels and water table depths greater than 10 m exist in more humid regions. Note that this is a pre-development simulation, thus, results do not include any anthropogenic water management features such as groundwater pumping, surface water reservoirs, irrigation or urbanization, although many of these anthropogenic impacts have been implemented into the ParFlow modeling framework (Ferguson and Maxwell, 2011; Condon and Maxwell, 2013, 2014). While anthropogenic impacts are clearly influential on water resources, a baseline simulation allows for a comparison between the altered and unaltered systems.

Figure 5 plots observed and simulated hydraulic head and streamflow for the dataset shown in Fig. 2. Hydraulic head (Fig. 5a) is plotted (as opposed to water table depth) as it is the motivating force for lateral flow in the simulation; it includes both the topography and pressure influences on the final solution. We see a very close agreement between observations and model simulations, though given the large range in hydraulic heads the goodness of fit may be somewhat obscured. Additional metrics and comparisons are explored below. Simulated streamflow (Fig. 5b) also agrees closely with observations. There is some bias, particularly for smaller flows, which also exhibit more scatter than larger flows, and may be due to the 1 km grid resolution employed here. Larger flows are more integrated measures of the system and might be less sensitive to resolution or local heterogeneity in model parameters.

GMDD
7, 7317–7349, 2014

CC BY

Figure 6 plots histograms of predicted and observed water table depth (a), hydraulic head (b), median (50th percentile) flow and 75th percentile flows (c and d). The hydraulic head shows good agreement between simulated and observed (Fig. 6b). While hydraulic head is the motivation for lateral flow and has been used in prior comparisons (e.g. Fan et al., 2007) both observed and simulated values are highly dependent on the local elevation. Figure 6a plots the water table depth below ground surface, or the difference between local elevation and groundwater. Here we see the simulated water table depths are shallower than the observed, something observed in prior simulations of large-scale water table depth (Fan et al., 2013). The observed water tables may include anthropogenic impacts, namely groundwater pumping, while the model simulations do not and this is a likely cause for this difference. Also, because groundwater wells are usually installed for extraction purposes there is no guarantee that the groundwater observations are an unbiased sample of the system as a whole. Figure 6c plots the steady-state derived flow values compared to median observed flow values and Fig. 6d plots these same steady-state simulated flows compared to the 75th percentile of the observed transient flow at each station. While the ParFlow model provides a robust representation of runoff generation processes, the steady-state simulations average event flows. We see the model predicts greater flow than the 50th percentile observed flows (Fig. 6c) and good agreement between the model simulations and the 75th percentile observed flows (Fig. 6d). This indicates a potentially wet bias in the forcing, which might also explain the shallower water table depths.

Figures 7 and 8 compare observed and simulated flows and water table depths for each of the major basin encompassed by the model. Water tables are generally predicted to be shallower in the model than observations with the exception of the Upper and Lower Colorado, which demonstrate better agreement between model simulations and observations than other basins. These histograms agree with a visual inspection of Figs. 2b and 4 which also indicate deeper observed water tables. Figure 8 indicates that simulated histograms of streamflow also predict more flow than the observations. This might indicate that the *P*-*E* forcing is too wet. However, a comparison of streamflow for

CC BY

the Colorado, where water table depths agree and flows are overpredicted, indicates a more complex set of interactions than basic water balance driven by forcing.

To better diagnose model processes, model inputs are compared with model simulation outputs over example regions chosen to isolate the impact of topographic slope, forcing and hydraulic conductivity on subsurface-surface water hydrodynamics. Figure 9 juxtaposes slope, potential recharge, surface flow, water table depth, hydraulic conductivity and a satellite image composite also at 1 km resolution (the NASA Blue Marble image, Justice et al., 2002) and facilitates a visual diagnosis of control by the three primary model inputs. While the model was run to steady-state and ultimately all the potential recharge has to exit the domain as discharge, the distribution and partitioning between groundwater and streams depends on the slope and hydraulic conductivity. Likewise, while topographic lows create the potential for flow convergence, it is not a model requirement that this create a stream. Figure 9 demonstrates some of these relationships quite clearly over a portion of the model that transitions from semi-arid to more humid conditions as the North and South Platte River systems join the Missouri. As expected changes in slope yield flow convergence, however, this figure also shows that as recharge increases from west to east ($X > 1700$ km, panel c) the model generally predicts shallower water tables and greater stream density (panels d and e, respectively). Conversely, in localized areas of decreased P-E (e.g. 700 km $< Y <$ 900 km specifically south of the Platte River) water tables increase and stream densities decrease. The satellite image (panel f) shows increases in vegetation that correspond to shallower water tables and increased stream density.

Hydraulic conductivity also has a significant impact on water table depth and, somewhat counter intuitively, stream network density. In areas of greater recharge in the eastern portion of Fig. 9c, regions with larger hydraulic conductivity (panel b) show decreased stream network density and increased water table depths. This more clearly demonstrated in Fig. 10 (a region in the upper Missouri) where, except for the northeast corner, recharge is uniformly low. Slopes are also generally low (panel a), yet hydraulic conductivities show a substantial increase due to a change in datasets between state

CC BY

and country boundaries (panel b, $X > 1250$ km, $Y > 1400$ km). The relative increase in hydraulic conductivity decreases hydraulic gradients under steady state conditions and generally increases water table depth, which in turn decreases stream network density. This change in hydraulic conductivity yields a decrease in the formation of stream networks resulting in an increase in water table depth. Thus, hydraulic conductivity has an important role in partitioning moisture between surface and subsurface flow, even under steady-state conditions. While mass balance requires that overall flow must be conserved, larger conductivity values allow this flow to be maintained within the subsurface while lower conductivities force the surface stream network to maintain this flow. In turn, stream networks connect regions of varying hydrodynamic conditions and may result in locally infiltrating conditions creating a losing-stream to recharge groundwater. This underscores the connection between input variables and model predictions, an equal importance of hydraulic conductivity to recharge in model states and the need to continually improve input datasets.

Finally, the connection between stream flow and drainage area is a classical scaling relationship (Rodriguez-Iturbe and Rinaldo, 2001), which usually takes the power law form $Q = kA^n$, where Q is volumetric streamflow [$L^3 T^{-1}$], A is the contributing upstream area [L^2] and k [$L T^{-1}$] and n are empirical constants. While this relationship has been demonstrated for individual basins and certain flow conditions (Rodriguez-Iturbe and Rinaldo, 2001), generality has not been established (Glaster, 2009). Figure 10a plots simulated streamflow as a function of associated drainage area on log-log axes, and Fig. 10b plots the same variables for median observed streamflow from more than 4000 gaging stations. While no single functional relationship is evident from this plot, there is a striking maximum limit of flow as a function of drainage area with a continental scaling coefficient of $n = 0.84$. Both Fig. 10a and b are colored by aridity index (AI), the degree of dryness of a given location. Color gradients that transition from blue (more humid) to red (more arid) show that humid basins fall along the maximum flow-discharge line, while arid basins have less discharge and fall below this line. For discharge observations (Fig. 10b) the same behavior is observed, where more humid stations fall along

GMDD
7, 7317–7349, 2014

cc BY

the $n = 0.9$ line and more arid stations fall below this line. Essentially this means that in humid locations, where water is not a limiting factor, streamflow scales most strongly with topography and area. Conversely arid locations fall below this line because flow to streams is limited by groundwater storage.

5 Conclusions

Here we present the results of an integrated, multiphysics-based hydrologic simulation covering much of Continental North America at hyperresolution (1 km). This simulation provides a consistent theoretical framework for the analysis of groundwater and surface water interactions and scaling from the headwaters to continental scale (10^0–10^7 km^2). The framework exploits high performance computing to meet this grand challenge in hydrology (Wood et al., 2011). We demonstrate that continental-scale, integrated hydrologic models are feasible and can reproduce observations and the essential features of streamflow and groundwater. Results show that scaling of surface flow is related to both drainage area and aridity. These results may be interrogated further to understand the role of topography, subsurface properties and climate on groundwater table and streamflow, and used as a platform to diagnose scaling behavior, e.g. surface flow from the headwaters to the continent.

These presented results are a first-step in high resolution, integrated, continental-scale simulation. We simulate an unaltered, or pre-development scenario of groundwater and surface water flows. As such, discussion focuses on the physical controls of groundwater surface water interactions and scaling behavior; however there are obvious limitations to this scenario. Clearly reservoir management, groundwater pumping, irrigation, diversion and urban expansion all shape modern hydrology. Additionally, the steady-state simulation does not take into consideration temporal dynamics or complex land-surface processes, also important in determining the quantity and fluxes of water. These limitations can all be addressed within the current modeling framework but require transient simulations and additional computational resources. Model performance

GMDD
7, 7317–7349, 2014

CC BY

is also limited by the quality of available input datasets. As noted throughout the discussion, existing datasets are subject to uncertainty and are clearly imperfect. As improved subsurface characterization becomes available this information can be used to better inform models. Though, the magnitudes of states and fluxes may change with improved datasets, the overall trends and responses predicted here are not likely to change. While there are always improvements to be made, these simulations represent a critical first step in understanding coupled surface subsurface hydrologic processes and scaling at large spatial extent.

This study highlights the utility of high performance computing in addressing the grand challenges in hydrological sciences and represents an important advancement in our understanding of hydrologic scaling in continental river basins. By providing an integrated model we open up a useful avenue of research to bridge physical processes across spatial scales in a hydrodynamic, physics-based upscaling framework.

Code availability

ParFlow is an open-source, modular, parallel integrated hydrologic platform freely available via the GNU LPGL license agreement. ParFlow is developed by a community led by the Colorado School of Mines and F-Z Jülich with contributors from a number of other institutions. Specific versions of ParFlow are archived with complete documentation and may be downloaded[1] or checked-out from a commercially hosted, free SVN repository. The input data and simulations presented here will be made available and may be obtained by contacting the lead author via email.

Acknowledgements. The authors wish to thank the Jülich Supercomputing Centre (JSC) for providing the compute time necessary for this work, VSR-Project #8308.

[1]http://inside.mines.edu/~rmaxwell/maxwell_software.shtml

Discussion Paper | Discussion Paper | Discussion Paper | Discussion Paper |

GMDD
7, 7317–7349, 2014

References

Anyah, R. O., Weaver, C. P., Miguez-Macho, G., Fan, Y., and Robock, A.: Incorporating water table dynamics in climate modeling: 3. Simulated groundwater influence on coupled land–atmosphere variability, J. Geophys. Res.-Atmos., 113, D07103, doi:10.1029/2007JD009087, 2008.

Ashby, S. F. and Falgout, R. D.: A parallel multigrid preconditioned conjugate gradient algorithm for groundwater flow simulations, Nucl. Sci. Eng., 124, 145–159, 1996.

Camporese, M., Paniconi, C., Putti, M., and Orlandini, S.: Surface-subsurface flow modeling with path-based runoff routing, boundary condition-based coupling, and assimilation of multisource observation data, Water Resour. Res., 46, W02512, doi:10.1029/2008wr007536, 2010.

Camporese, M., Penna, D., Borga, M., and Paniconi, C.: A field and modeling study of nonlinear storage-discharge dynamics for an alpine headwater catchment, Water Resour. Res., 50, 806–822, doi:10.1002/2013wr013604, 2014.

Condon, L. E. and Maxwell, R. M.: Implementation of a linear optimization water allocation algorithm into a fully integrated physical hydrology model, Adv. Water. Resour., 60, 135–147, doi:10.1016/j.advwatres.2013.07.012, 2013.

Condon, L. E. and Maxwell, R. M.: Feedbacks between managed irrigation and water availability: diagnosing temporal and spatial patterns using an integrated hydrologic model, Water Resour. Res., 50, 2600–2616, doi:10.1002/2013wr014868, 2014.

Condon, L. E., Maxwell, R. M., and Gangopadhyay, S.: The impact of subsurface conceptualization on land energy fluxes, Adv. Water. Resour., 60, 188–203, doi:10.1016/j.advwatres.2013.08.001, 2013.

Döll, P., Hoffmann-Dobrev, H., Portmann, F. T., Siebert, S., Eicker, A., Rodell, M., Strassberg, G., and Scanlon, B. R.: Impact of water withdrawals from groundwater and surface water on continental water storage variations, J. Geodyn., 59–60, 143–156, 2012.

Fan, Y., Miguez-Macho, G., Weaver, C. P., Walko, R., and Robock, A.: Incorporating water table dynamics in climate modeling: 1. water table observations and equilibrium water table simulations, J. Geophys. Res.-Atmos., 112, D10125, doi:10.1029/2006JD008111, 2007.

Fan, Y., Li, H., and Miguez-Macho, G.: Global patterns of groundwater table depth, Science, 339, 940–943, doi:10.1126/science.1229881, 2013.

Ferguson, I. M. and Maxwell, R. M.: Hydrologic and land–energy feedbacks of agricultural water management practices, Environ. Res. Lett., 6, 014006, doi:10.1088/1748-9326/6/1/014006, 2011.
Freeze, R. A. and Harlan, R. L.: Blueprint for a phyiscally-based, digitally-simulated hydrologic response model, J. Hydrol., 9, 237–258, 1969.
Glaster, J. C.: Testing the linear relationship between peak annual river discharge and drainage area using long-term usgs river gauging records, Geol. S. Am. S., 451, 159–171, doi:10.1130/2009.2451(11), 2009.
Gleeson, T. and Cardiff, M.: The return of groundwater quantity: a mega-scale and interdisciplinary "future of hydrogeology"?, Hydrogeol. J., 21, 1169–1171, doi:10.1007/s10040-013-0998-8, 2014.
Gleeson, T., Marklund, L., Smith, L., and Manning, A. H.: Classifying the water table at regional to continental scales, Geophys. Res. Lett., 38, L05401, doi:10.1029/2010GL046427, 2011a.
Gleeson, T., Smith, L., Moosdorf, N., Hartmann, J., Dürr, H. H., Manning, A. H., van Beek, L. P. H., and Jellinek, A. M.: Mapping permeability over the surface of the earth, Geophys. Res. Lett., 38, L02401, doi:10.1029/2010gl045565, 2011b.
Goderniaux, P., Brouyère, S., Fowler, H. J., Blenkinsop, S., Therrien, R., Orban, P., and Dassargues, A.: Large scale surface–subsurface hydrological model to assess climate change impacts on groundwater reserves, J. Hydrol., 373, 122–138, doi:10.1016/j.jhydrol.2009.04.017, 2009.
Jiang, X., Niu, G. Y., and Yang, Z. L.: Impacts of vegetation and groundwater dynamics on warm season precipitation over the central united states, J. Geophys. Res., 114, D06109, doi:10.1029/2008JD010756, 2009.
Jones, J. E. and Woodward, C. S.: Newton-krylov-multigrid solvers for large-scale, highly heterogeneous, variably saturated flow problems, Adv. Water. Resour., 24, 763–774, 2001.
Jones, J. P., Sudicky, E. A., Brookfield, A. E., and Park, Y. J.: An assessment of the tracer-based approach to quantifying groundwater contributions to streamflow, Water Resour. Res., 42, W02407, doi:10.1029/2005wr004130, 2006.
Jones, J. P., Sudicky, E. A., and McLaren, R. G.: Application of a fully-integrated surface-subsurface flow model at the watershed-scale: a case study, Water Resour. Res., 44, W03407, doi:10.1029/2006wr005603, 2008.

GMDD
7, 7317–7349, 2014

Justice, C. O., Townshend, J. R. G., Vermote, E. F., Masuoka, E., Wolfe, R. E., Saleous, N., Roy, D. P., and Morisette, J. T.: An overview of modis land data processing and product status, Remote. Sens. Environ., 83, 3–15, doi:10.1016/S0034-4257(02)00084-6, 2002.

Kollet, S. J. and Maxwell, R. M.: Integrated surface-groundwater flow modeling: a free-surface overland flow boundary condition in a parallel groundwater flow model, Adv. Water. Resour., 29, 945–958, 2006.

Kollet, S. J. and Maxwell, R. M.: Capturing the influence of groundwater dynamics on land surface processes using an integrated, distributed watershed model, Water Resour. Res., 44, W02402, doi:10.1029/2007WR006004, 2008.

Kollet, S. J., Cvijanovic, I., Schüttemeyer, D., Maxwell, R. M., Moene, A. F., and Bayer, P.: The influence of rain sensible heat, subsurface heat convection and the lower temperature boundary condition on the energy balance at the land surface, Vadose. Zone. J., 8, 846–857, 2009.

Kollet, S. J., Maxwell, R. M., Woodward, C. S., Smith, S., Vanderborght, J., Vereecken, H., and Simmer, C.: Proof of concept of regional scale hydrologic simulations at hydrologic resolution utilizing massively parallel computer resources, Water Resour. Res., 46, W04201, doi:10.1029/2009wr008730, 2010.

Kumar, M., Duffy, C. J., and Salvage, K. M.: A second order accurate, finite volume based, integrated hydrologic modeling (FIHM) framework for simulation of surface and subsurface flow, Vadose. Zone. J., 8, 873–890, doi:10.2136/vzj2009.0014, 2009.

Maurer, E. P., Wood, A. W., Adam, J. C., Lettenmaier, D. P., and Nijssen, B.: A long-term hydrologically based dataset of land surface fluxes and states for the conterminous united states*, J. Climate, 15, 3237–3251, doi:10.1175/1520-0442(2002)015<3237:althbd>2.0.CO;2, 2002.

Maxwell, R. M.: A terrain-following grid transform and preconditioner for parallel, large-scale, integrated hydrologic modeling, Adv. Water. Resour., 53, 109–117, doi:10.1016/j.advwatres.2012.10.001, 2013.

Maxwell, R. M. and Kollet, S. J.: Interdependence of groundwater dynamics and land-energy feedbacks under climate change, Nat. Geosci., 1, 665–669, 2008.

Maxwell, R. M., Chow, F. K., and Kollet, S. J.: The groundwater-land-surface-atmosphere connection: soil moisture effects on the atmospheric boundary layer in fully-coupled simulations, Adv. Water. Resour., 30, 2447–2466, doi:10.1016/j.advwatres.2007.05.018, 2007.

GMDD

7, 7317–7349, 2014

Simulation of groundwater and surface water over the continental

R. M. Maxwell et al.

CC BY

Maxwell, R. M., Lundquist, J. D., Mirocha, J. D., Smith, S. G., Woodward, C. S., and Tompson, A. F. B.: Development of a coupled groundwater-atmospheric model, Mon. Weather. Rev., 139, 96–116, doi:10.1175/2010MWR3392, 2011.
Maxwell, R. M., Putti, M., Meyerhoff, S., Delfs, J.-O., Ferguson, I. M., Ivanov, V., Kim, J., Kolditz, O., Kollet, S. J., Kumar, M., Lopez, S., Niu, J., Paniconi, C., Park, Y.-J., Phanikumar, M. S., Shen, C., Sudicky, E. A., and Sulis, M.: Surface-subsurface model intercomparison: a first set of benchmark results to diagnose integrated hydrology and feedbacks, Water Resour. Res., 50, 1531–1549, doi:10.1002/2013wr013725, 2014.
Miguez-Macho, G., Fan, Y., Weaver, C. P., Walko, R., and Robock, A.: Incorporating water table dynamics in climate modeling: 2. formulation, validation, and soil moisture simulation, J. Geophys. Res.-Atmos., 112, D13108, doi:10.1029/2006JD008112, 2007.
Mikkelson, K. M., Maxwell, R. M., Ferguson, I., Stednick, J. D., McCray, J. E., and Sharp, J. O.: Mountain pine beetle infestation impacts: modeling water and energy budgets at the hill-slope scale, Ecohydrology, 6, 64–72, doi:10.1002/eco.278, 2013.
Nir, Y. K., Haibin, L., and Ying, F.: Groundwater flow across spatial scales: importance for climate modeling, Environ. Res. Lett., 9, 034003, doi:10.1088/1748-9326/9/3/034003, 2014.
Osei-Kuffuor, D., Maxwell, R. M., and Woodward, C. S.: Improved numerical solvers for implicit coupling of subsurface and overland flow, Adv. Water. Resour., 77, 185–195, doi:10.1016/j.advwatres.2014.09.006, 2014.
Qu, Y. and Duffy, C. J.: A semidescrete finite volume formulation for multiprocess watershed simulation, Water Resour. Res., 43, W08419, doi:10.1029/2006WR005752, 2007.
Richards, L. A.: Capillary conduction of liquids in porous mediums, Physics, 1, 318–333, 1931.
Rihani, J. F., Maxwell, R. M., and Chow, F. K.: Coupling groundwater and land surface processes: idealized simulations to identify effects of terrain and subsurface heterogeneity on land surface energy fluxes, Water Resour. Res., 46, 1–14, doi:10.1029/2010WR009111, 2010.
Rodell, M., Velicogna, I., and Famiglietti, J. S.: Satellite-based estimates of groundwater depletion in india, Nature, 460, 999–1002, 2009.
Rodriguez-Iturbe, I. and Rinaldo, A.: Fractal river basins: chance and self-organization, Cambridge University Press, 2001.
Schaap, M. G. and Leij, F. J.: Database-related accuracy and uncertainty of pedotransfer functions, Soil. Sci., 163, 765–779, 1998.

Discussion Paper | Discussion Paper | Discussion Paper | Discussion Paper |

CC BY

Shi, Y., Davis, K. J., Duffy, C. J., and Yu, X.: Development of a coupled land surface hydrologic model and evaluation at a critical zone observatory, J. Hydrometeorol., 14, 1401–1420, doi:10.1175/jhm-d-12-0145.1, 2013.

Sudicky, E., Jones, J., Park, Y.-J., Brookfield, A., and Colautti, D.: Simulating complex flow and transport dynamics in an integrated surface-subsurface modeling framework, Geosci. J., 12, 107–122, doi:10.1007/s12303-008-0013-x, 2008.

Sulis, M., Paniconi, C., Marrocu, M., Huard, D., and Chaumont, D.: Hydrologic response to multimodel climate output using a physically based model of groundwater/surface water interactions, Water Resour. Res., 48, W12510, doi:10.1029/2012wr012304, 2012.

Taylor, R. G., Scanlon, B., Doll, P., Rodell, M., van Beek, R., Wada, Y., Longuevergne, L., Leblanc, M., Famiglietti, J. S., Edmunds, M., Konikow, L., Green, T. R., Chen, J., Taniguchi, M., Bierkens, M. F. P., MacDonald, A., Fan, Y., Maxwell, R. M., Yechieli, Y., Gurdak, J. J., Allen, D. M., Shamsudduha, M., Hiscock, K., Yeh, P. J. F., Holman, I., and Treidel, H.: Ground water and climate change, Nature Climate Change, 3, 322–329, doi:10.1038/nclimate1744, 2013.

Therrien, R., Sudicky, E., Park, Y., and McLaren, R.: Hydrogeosphere: A three-dimensional numerical modelling describing fully-integrated subsurface and surface flow and transport, User guide, Waterloo, Ontario, Canada, Aquanty Inc., 2012.

VanderKwaak, J. E. and Loague, K.: Hydrologic-response simulations for the r-5 catchment with a comprehensive physics-based model, Water Resour. Res., 37, 999–1013, 2001.

van Genuchten, M. T.: A closed-form equation for predicting the hydraulic conductivity of unsaturated soils, Soil. Sci. Soc. Am. J., 44, 892–898, 1980.

Williams, J. L. and Maxwell, R. M.: Propagating subsurface uncertainty to the atmosphere using fully-coupled, stochastic simulations, J. Hydrometeorol., 12, 690–701, doi:10.1175/2011JHM1363.1, 2011.

Wood, B. D.: The role of scaling laws in upscaling, Adv. Water. Resour., 32, 723–736, doi:10.1016/j.advwatres.2008.08.015, 2009.

Wood, E. F., Roundy, J. K., Troy, T. J., van Beek, L. P. H., Bierkens, M. F. P., Blyth, E., de Roo, A., Döll, P., Ek, M., Famiglietti, J., Gochis, D., van de Giesen, N., Houser, P., Jaffé, P. R., Kollet, S., Lehner, B., Lettenmaier, D. P., Peters-Lidard, C., Sivapalan, M., Sheffield, J., Wade, A., and Whitehead, P.: Hyperresolution global land surface modeling: meeting a grand challenge for monitoring earth's terrestrial water, Water Resour. Res., 47, W05301, doi:10.1029/2010wr010090, 2011.

CC BY

Xia, Y., Mitchell, K., Ek, M., Cosgrove, B., Sheffield, J., Luo, L., Alonge, C., Wei, H., Meng, J., Livneh, B., Duan, Q., and Lohmann, D.: Continental-scale water and energy flux analysis and validation for north american land data assimilation system project phase 2 (nldas-2): 2. Validation of model-simulated streamflow, J. Geophys. Res.-Atmos., 117, D03110, doi:10.1029/2011jd016051, 2012.

CC BY

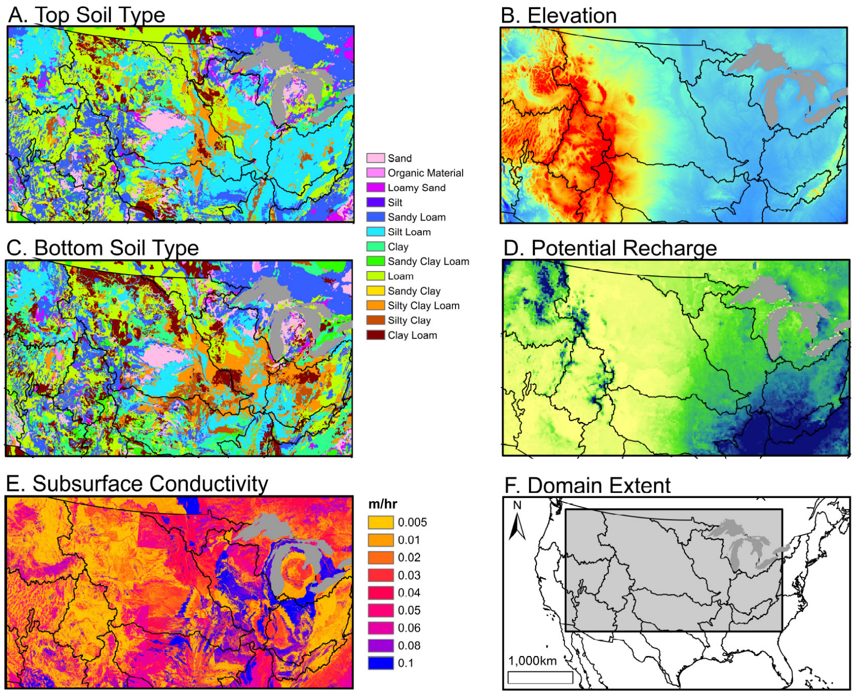

Figure 1. Maps of top soil type **(a)**, elevation (m a.s.l.) **(b)**, bottom soil type **(c)**, potential recharge, P-E, ($\mathrm{m\,y^{-1}}$) **(d)**, saturated hydraulic conductivity ($\mathrm{m\,h^{-1}}$) **(e)** over the model domain **(f)**.

GMDD
7, 7317–7349, 2014

Title Page
Abstract Introduction
Conclusions References
Tables Figures
◀ ▶
Back Close
Full Screen / Esc
Printer-friendly Version
Interactive Discussion

CC BY

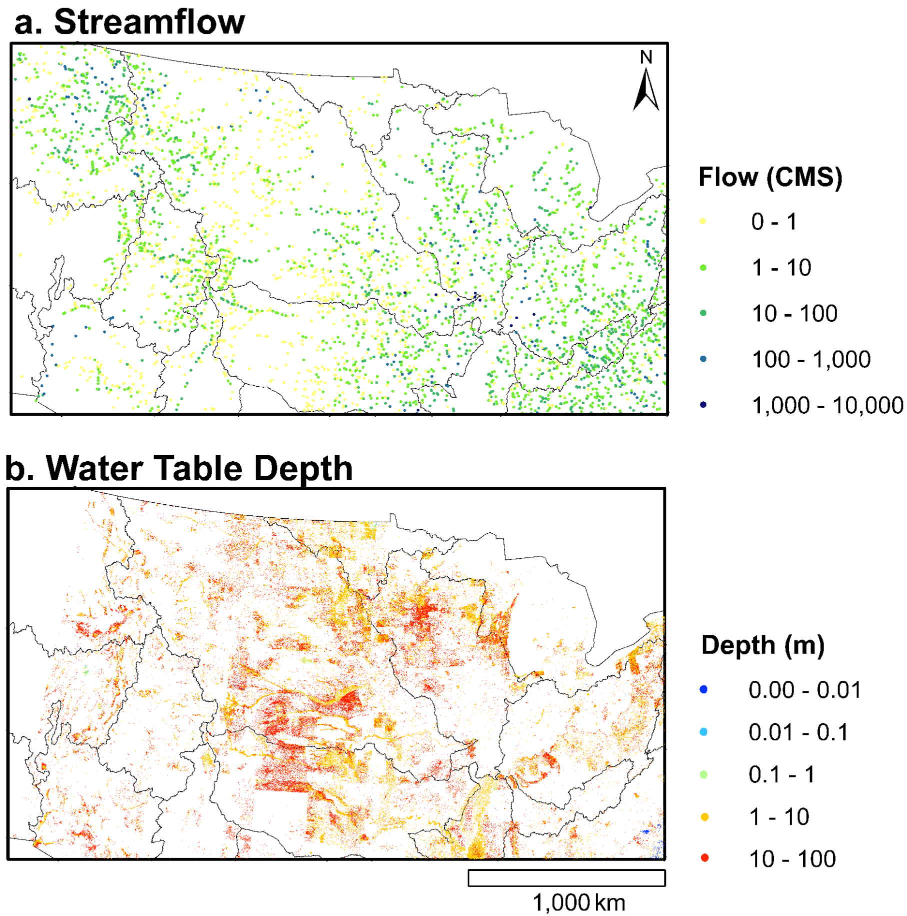

Figure 2. Plot of observed streamflow **(a)** and observed water table depth **(b)**.

GMDD
7, 7317–7349, 2014

Simulation of groundwater and surface water over the continental

R. M. Maxwell et al.

Title Page
Abstract Introduction
Conclusions References
Tables Figures
Back Close
Full Screen / Esc
Printer-friendly Version
Interactive Discussion

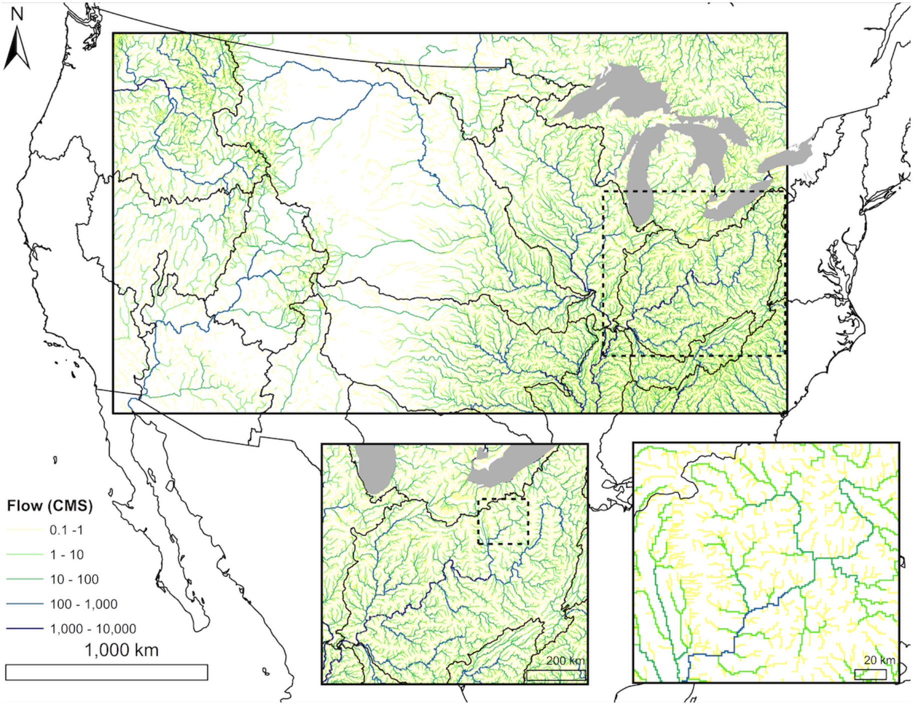

Figure 3. Map of simulated surface flow ($m^3 s^{-1}$) over the CONUS domain with two insets zooming into the Ohio river basin. Colors represent surface flow in log scale and line widths vary slightly with flow for the first two panels.

GMDD
7, 7317–7349, 2014

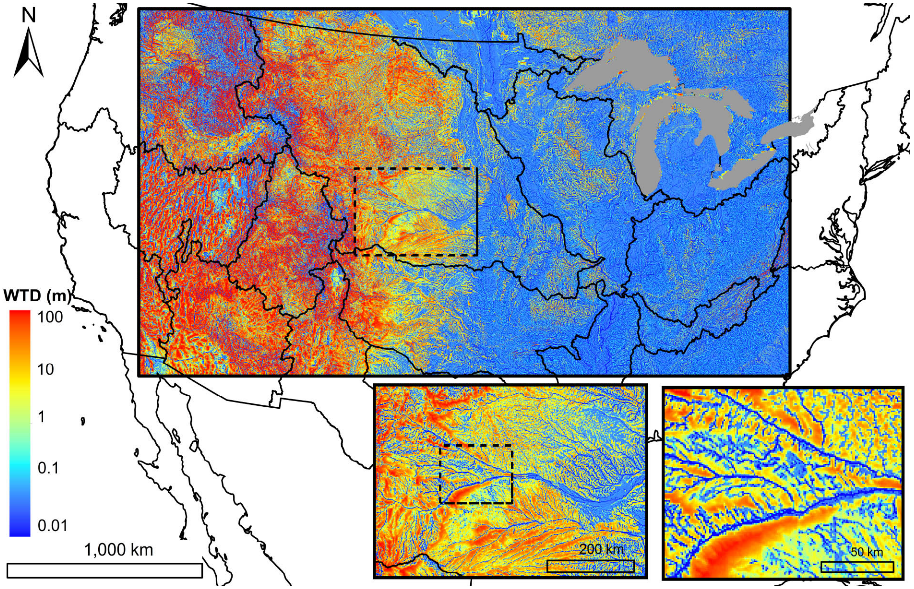

Figure 4. Map of water table depth (m) over the simulation domain with two insets zooming into the North and South Platte River basin, headwaters to the Mississippi. Colors represent depth in log scale (from 0.01 to 100 m).

GMDD
7, 7317–7349, 2014

Title Page
Abstract Introduction
Conclusions References
Tables Figures
◀| |▶
◀ ▶
Back Close
Full Screen / Esc
Printer-friendly Version
Interactive Discussion

CC BY

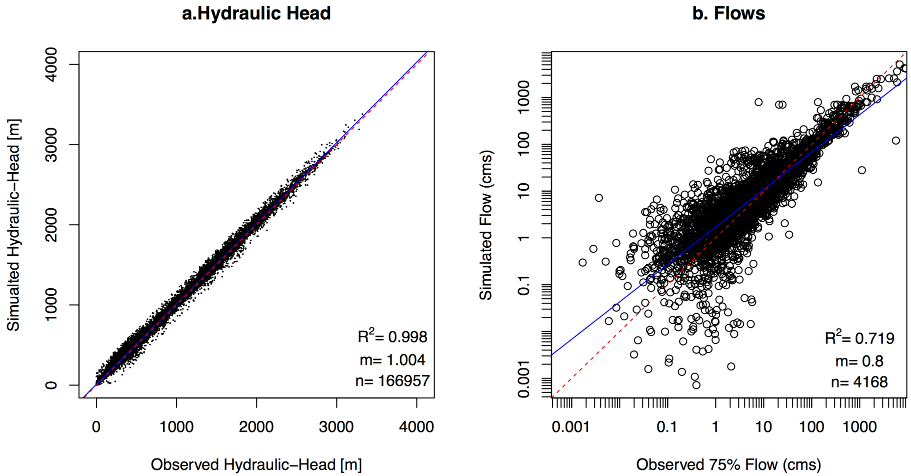

Figure 5. Scatterplots of simulated v. observed hydraulic head **(a)** and surface flow **(b)**.

GMDD
7, 7317–7349, 2014

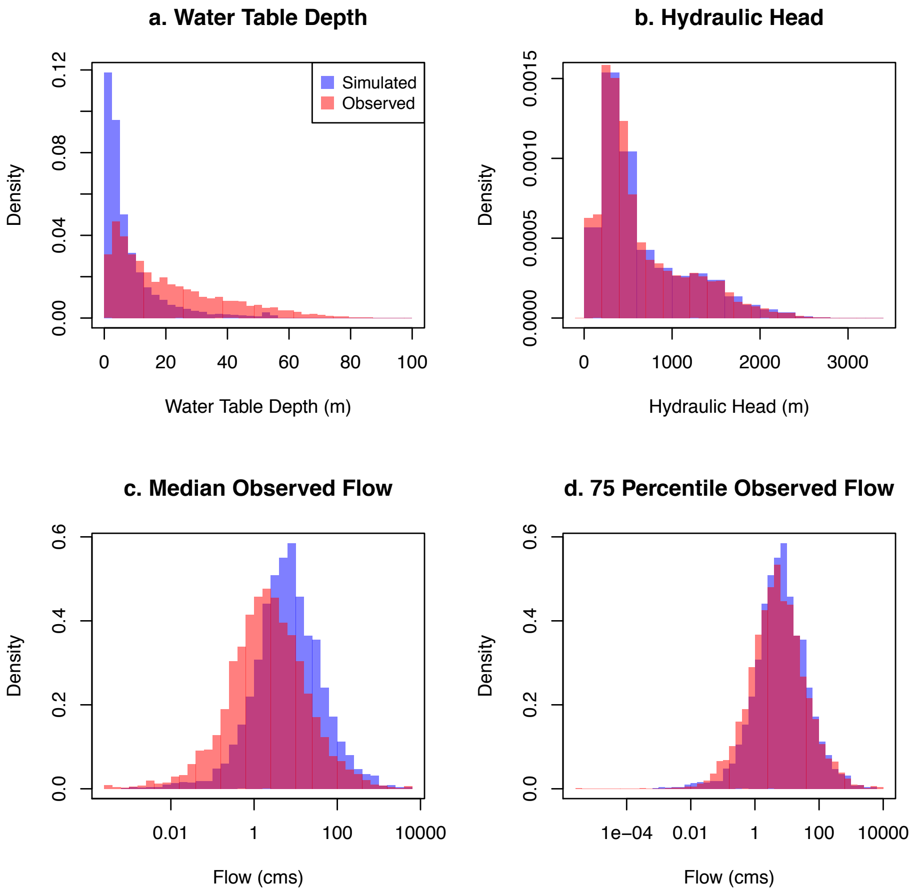

Figure 6. Histograms of simulated and observed water table depth **(a)**, hydraulic head **(b)**, median observed flow **(c)** and 75th percentile observed flow **(d)**.

GMDD
7, 7317–7349, 2014

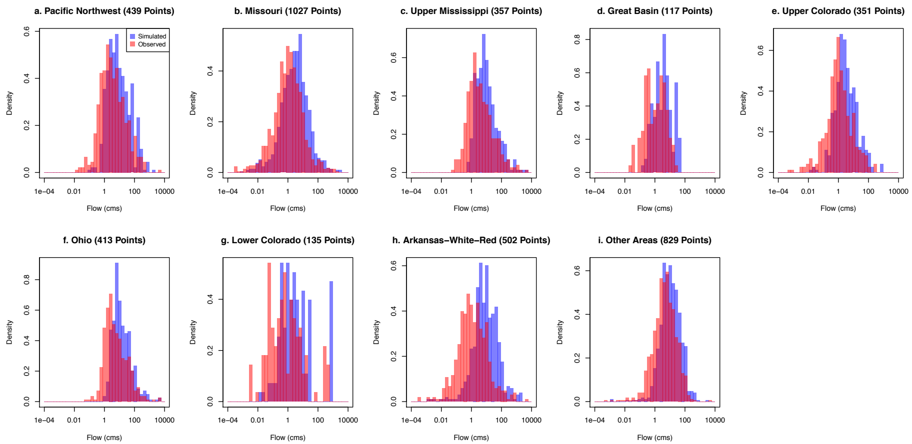

Figure 7. Distributions of observed and simulated streamflow by basin as indicated.

GMDD
7, 7317–7349, 2014

Simulation of groundwater and surface water over the continental

R. M. Maxwell et al.

CC BY

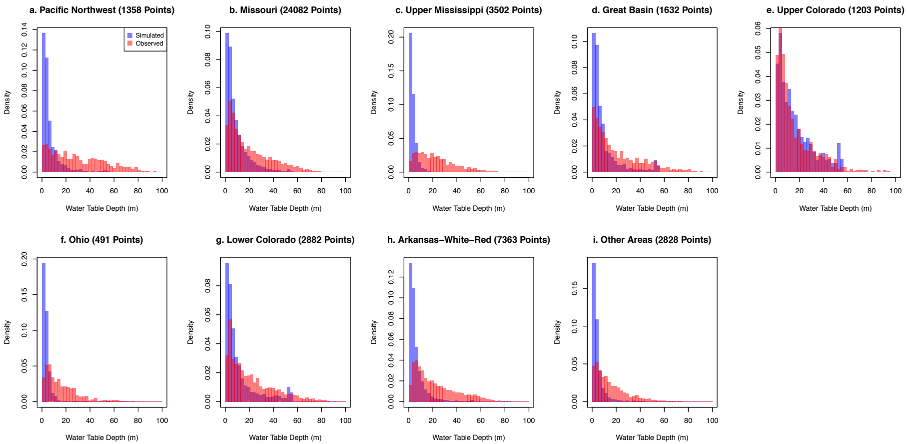

Figure 8. Distributions of observed and simulated water table depth by basin as indicated.

GMDD
7, 7317–7349, 2014

CC BY

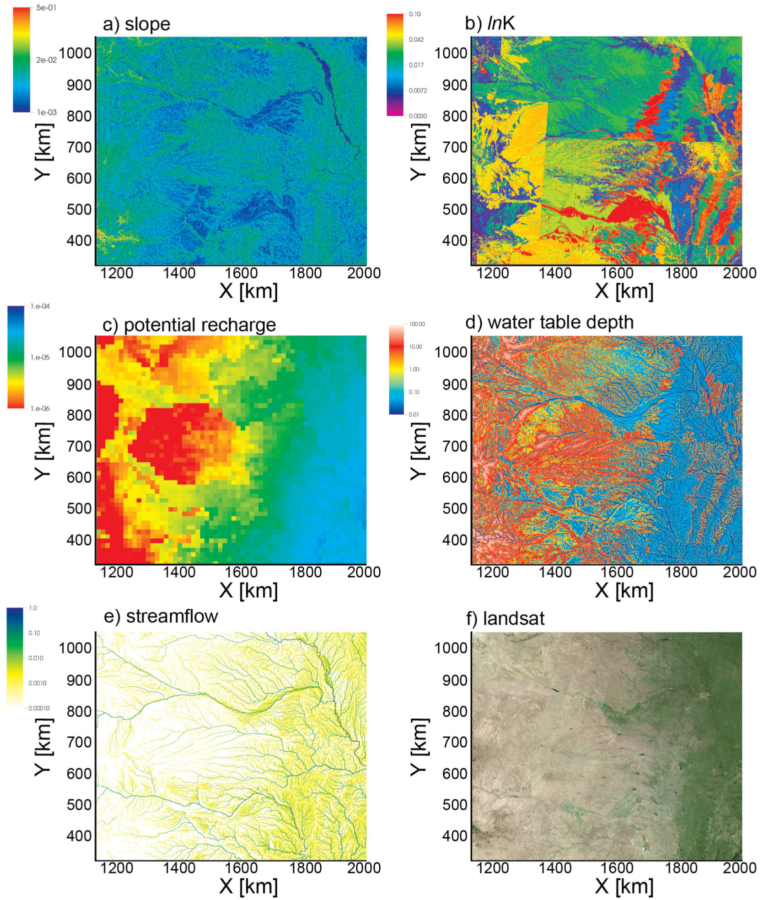

Figure 9. Plots of topographic slope **(a)**, hydraulic conductivity **(b)** potential recharge **(c)**, water table depth **(d)**, streamflow **(e)** and satellite image **(f)** for a region of the model covering the Platte River basin.

CC BY

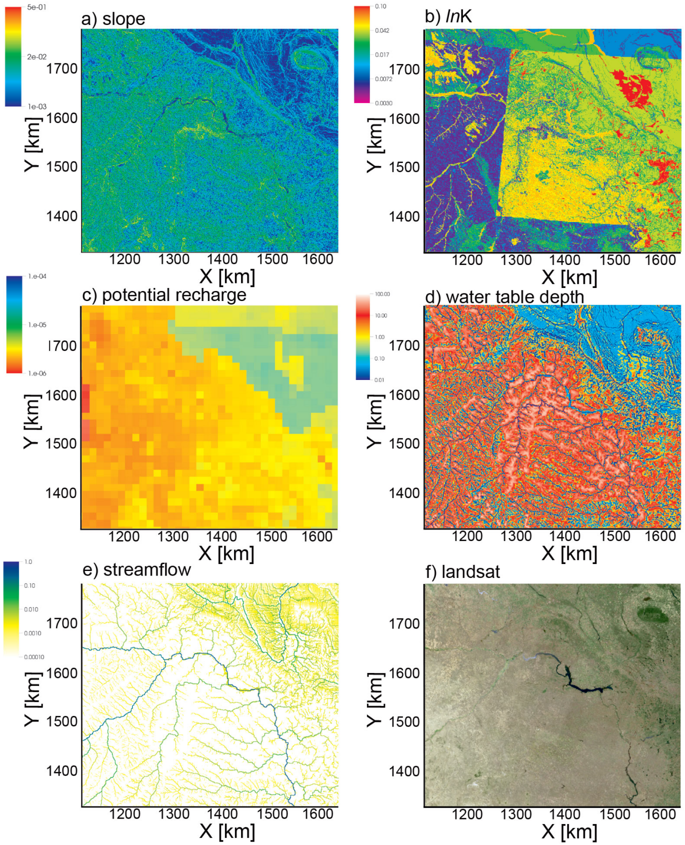

Figure 10. Plots of topographic slope **(a)**, hydraulic conductivity **(b)** potential recharge **(c)**, water table depth **(d)**, streamflow **(e)** and satellite image **(f)** for a region of the model covering the Upper Missouri basin.

CC BY

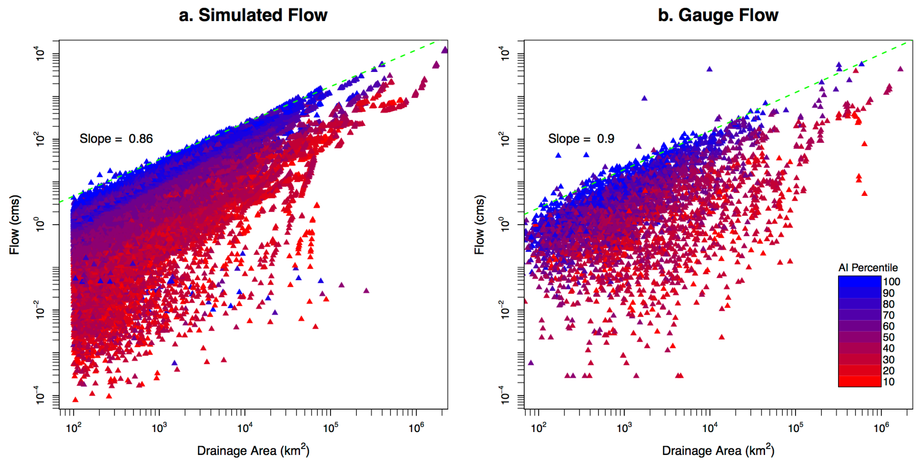

Figure 11. Plots of scaling relationships for simulated and median observed surface flow. Log-scale plots of surface flow as a function of contributing drainage area derived from the model simulation **(a)** and observations **(b)**. Individual symbols are colored by aridity index (AI) with blue colors being humid and red colors being arid in panels **(a)** and **(b)**.

GMDD
7, 7317–7349, 2014

Simulation of groundwater and surface water over the continental

R. M. Maxwell et al.